

# Multi-Modal Film Boiling Simulations on Adaptive Octree Grids

M. Wasy Akhtar

**Abstract**—Multi-modal film boiling simulations are carried out on adaptive octree grids. The liquid-vapor interface is captured using the volume-of-fluid framework adjusted to account for exchanges of mass, momentum, and energy across the interface. Surface tension effects are included using a volumetric source term in the momentum equations. The phase change calculations are conducted based on the exact location and orientation of the interface; however, the source terms are calculated using the mixture variables to be consistent with the one field formulation used to represent the entire fluid domain. The numerical model on octree representation of the computational grid is first verified using test cases including advection tests in severely deforming velocity fields, gravity-based instabilities and bubble growth in uniformly superheated liquid under zero gravity. The model is then used to simulate both single and multi-modal film boiling simulations. The octree grid is dynamically adapted in order to maintain the highest grid resolution on the instability fronts using markers of interface location, volume fraction, and thermal gradients. The method thus provides an efficient platform to simulate fluid instabilities with or without phase change in the presence of body forces like gravity or shear layer instabilities.

**Keywords**—Boiling flows, dynamic octree grids, heat transfer, interface capturing, phase change.

## NOMENCLATURE

### Letters

$A$	Amplitude ( $m$ )
$A_f$	Area side fraction
$\left(\frac{A_{\text{inter}}}{V_{\text{cell}}}\right)$	Area of the interface to cell volume ratio ( $1/m$ )
$c$	Mixture (mass-averaged) constant pressure specific heat ( $J/kg/K$ )
$g$	Gravitational acceleration ( $m/s^2$ )
$h$	Enthalpy ( $J/kg$ )
$h_{fg}$	Enthalpy of phase change ( $J/kg$ )
$k$	Thermal conductivity ( $W/m^2 K$ )
$l_s$	Length scale
$L$	Latent heat of vaporization ( $J/kg$ )
$\dot{m}''$	Mass flux per unit area across the interface ( $kg/s/m^2$ )
$N$	Number of Fourier terms
$n$	Unit normal vector to interface
$n_x$	Number of modes of the perturbation
$P$	Volume averaged mixture pressure ( $N/m^2$ )
$\vec{q}$	Heat flux vector ( $W/m^2$ )
$r$	Random number
$S_{\text{energy}}$	Energy source term associated with phase change ( $W/m^3$ )
$S_{\text{mom,pc}}$	Momentum source term associated with phase change ( $N/m^3$ )

$S_{\text{mom,st}}$	Momentum source term associated with surface tension ( $N/m^3$ )
$T$	Mass averaged mixture temperature ( $K$ )
$\Delta T$	Superheat ( $K$ )
$t$	Time ( $s$ )
$t_s$	time scale
$u$	Mixture fluid velocity ( $m/s$ )
$u_s$	velocity scale
$W$	Domain width ( $m$ )
$y$	Interface height
$z$	Interface height

### Greek Letters

$\alpha$	Volume fraction
$\varepsilon$	Perturbation constant
$\lambda$	Wavelength ( $m$ )
$\mu$	Dynamic viscosity
$\nu$	Kinematic viscosity
$\rho$	Volume averaged mixture density ( $kg/m^3$ )
$\sigma$	Surface tension ( $N/m$ )
$\tau$	Volume averaged mixture shear stress ( $N/m^2$ )

### Subscripts

$c$	Critical value
$cell$	Value of the computational cell
$d2$	Value for the two-dimensional problem
$d3$	Value for the three-dimensional problem
$f$	Value at cell face
$l$	Value for the liquid phase
$mom$	Value associated with momentum
$pc$	Value associated with phase change
$sat$	Value for saturation condition
$st$	Value associated with surface tension
$v$	Value for vapor phase
$w$	Value at the wall

## I. INTRODUCTION

COMPUTATION of boiling flows is one of the most challenging problems in computational fluid dynamics not only because two distinct phases must be modeled with correct accounting of surface tension and interfacial discontinuities, but a wide range of scales must be resolved both spatially and temporally. The problem is further complicated by the mass exchange between the phases and the need to solve at least one additional equation in order to capture/track the liquid-vapor interface. Also, the interface temperature condition can be a function of the heat flux at the interface, which requires additional modeling effort to set the right temperature.

Given the spatial resolution and grid quality required to simulate such problems, a uniform grid is highly desirable and almost required in order to maintain the accuracy of the

M. W. Akhtar was with the University of Houston, Houston, TX 77204 USA (e-mail: mwakhtar3@uh.edu).

interface reconstruction algorithm. Some of the early and pioneering works done in the computation of boiling flows by Tryggvason and others have primarily used uniform grids, but these can be computationally expensive. Most of the simulations of boiling flows are conducted in two-dimensional planar or axi-symmetric domains in order to keep the simulation times reasonable. The work presented below uses a sharp interface capturing scheme within the volume-of-fluid (VOF) framework on an octree-based grid structure where the grid can be dynamically adapted based on the gradients of flow variables, interface location and curvature. The framework described is suitable for creating fully three-dimensional models. A set of test cases including Rayleigh Taylor instability, Enright deformation (vortex in a box) test case and spherical bubble growth are used to validate the interface capturing scheme and phase change model on an octree platform. The validated model is then used to conduct film boiling simulations in both single and multi-modes.

## II. NUMERICAL METHOD

Details of the interface tracking scheme are documented in [1]. In brief, the Navier-Stokes and energy equations are solved in terms of mixture variables as listed below:

$$\frac{\partial \rho}{\partial t} + \nabla \cdot (\rho \vec{u}) = 0 \quad (1)$$

$$\frac{\partial (\rho \vec{u})}{\partial t} + \nabla \cdot (\rho \vec{u} \vec{u}) = -\nabla p + \rho \vec{g} + \nabla \cdot \vec{\tau} + \vec{S}_{mom,st} + \vec{S}_{mom,pc} \quad (2)$$

$$\frac{\partial (\rho c T)}{\partial t} + \nabla \cdot (\rho \vec{u} c T) = -\nabla \cdot \vec{q} + \nabla \cdot \vec{\tau} + S_{energy} \quad (3)$$

Here, the mixture variables including density ( $\rho$ ), viscosity ( $\mu$ ) and pressure ( $p$ ) are volume-averaged, whereas the thermal variables like specific heat are mass-averaged. The surface tension jump across the interface is modeled as a volumetric source term based on the model of [2]. The source term  $\vec{S}_{mom,pc}$  is the volumetric source term to account for momentum exchange between the phases. The source term,  $S_{energy}$  is a volumetric source term to account for energy exchange between liquid and vapor due to phase change and is expressed as:

$$S_{energy} = -\dot{m}'' L (A_{int}/V_{cell}) = (\vec{q}_v - \vec{q}_l) \cdot \vec{n}_l (A_{int}/V_{cell}) \\ = (-k_l \nabla T_l + k_v \nabla T_v) \cdot \vec{n}_l (A_{int}/V_{cell}) \quad (4)$$

In addition to the mixture conservation equations, an additional equation to capture the interface is solved as:

$$\frac{\partial (\rho_v \alpha_v)}{\partial t} + \nabla \cdot (\rho_v \alpha_v \vec{u}_v) = \dot{m}'' \left( \frac{A_{int}}{V_{cell}} \right) \quad (5)$$

This describes a one-cell thick moving interface with a volume fraction of 0.5 within the VOF framework to capture/

track the liquid-vapor interface. The VOF field, once solved, needs to be reconstructed to locate the position and orientation of the interface. Details of the reconstruction scheme are in [3].

## III. COMPUTATIONAL GRID

An octree-based grid structure is used to solve the mass, momentum, and energy conservation equations and the interface advection equation. A uniform parent grid is dynamically adapted based on gradients of flow variables and the volume fraction gradient. The quartering of the parent into child grids maintains the accuracy of the interface reconstruction scheme by preserving a cell aspect ratio of unity. A schematic of the adapted grid and its corresponding tree representation is shown in Fig. 1.

## IV. NUMERICAL PROCEDURE

The set of conservation equations is solved using ANSYS Fluent<sup>TM</sup> (version 15.0). The advection term for the momentum equations is discretized using a Quadratic Upwind Interpolation for Convective Kinetics (QUICK) scheme, whereas the diffusion terms are discretized using central differences. The unsteady term is discretized using a first order Euler scheme. The results are thus first order accurate in time and at least second order in space. Pressure-velocity coupling is done using the Pressure Implicit with Splitting of Operator (PISO) scheme. More details of the solution procedure including a flowchart can be found in [4]. The algebraic equations obtained after discretization are iteratively solved using the Gauss-Seidel method. Convergence of the iterative solver is enhanced using the Algebraic Multigrid Method (AMG). The residuals for continuity, momentum and energy equations are set to  $10^{-4}$ ,  $10^{-5}$  and  $10^{-6}$ , respectively.

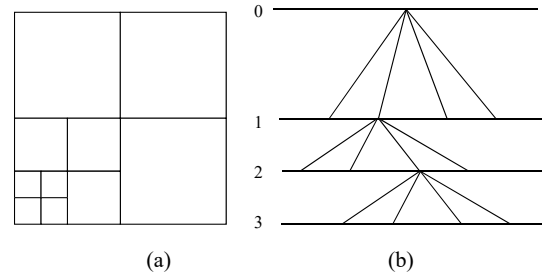


Fig. 1 (a) Octree grid schematic and (b) corresponding tree representation

## V. RESULTS

### A. Test Cases

A suite of test cases including Rayleigh Taylor instability, Enright deformation test, and spherical bubble growth in a uniform superheated liquid are used to validate the model. The Rayleigh Taylor instability demonstrates the high fidelity with which the numerical model can simulate the growth of a perturbed interface under the action of normal gravity conditions into self-similar mushroom-like structures. The

Enright deformation test validates the accuracy of the advection scheme in terms of maintaining thin filaments under the action of a single vortex; when the direction of the vortex is reversed in time, the model should return to the initial prescribed shape (a sphere). The final test case, spherical bubble growth in a uniform superheated liquid, validates the phase change model in terms of bubble radius as a function of time in the “diffusion-limited” regime. These results are documented in [3].

Once validated, the model is then used to compute single and multi-modal film boiling simulations, which demonstrate the accuracy and efficiency of the model for one of the most complex problems with a wide range of spatial scales that require high fidelity.

### B. Film Boiling Configuration

Film boiling from a flat surface is studied after perturbing the liquid-vapor interface with a sinusoidal function. The heated wall is considered to be horizontal with periodic boundary conditions. The thermo-physical properties that characterize film boiling are captured by the following non-dimensional groups:

- Grashof number  $Gr = \rho_v (\rho_l - \rho_v) g l_s^3 / \nu^2$ ,
- Jakob number  $Ja = c_v \Delta T / h_{fg}$  or  $q_w / \rho_v u_s h_{fg}$ ,
- Prandtl number  $Pr_v = \mu_v c_{p,v} / k_v$ .

The length scale for the problem is defined to be the capillary length scale  $l_s = \sqrt{\sigma / (\rho_l - \rho_v) g}$ ; the velocity and time scales are defined using the acceleration due to gravity as  $u_s = \sqrt{l_s g}$  and  $t_s = \sqrt{l_s / g}$ , respectively. In addition to the above non-dimensional numbers, the ratio of material properties like density, viscosity, thermal conductivity, and specific heat are also specified, in order to have a unique boiling configuration.

The most critical wavelength for film boiling is given by  $\lambda_c = 2\pi l_s$ . In two dimensions, the most unstable Taylor wavelength is given by  $\lambda_{d2} = 2\pi\sqrt{3}l_s$ . The most critical Taylor wavelength in three-dimensions,  $\lambda_{d3}$ , is related to the one in two-dimensions by  $(\lambda_{d3} = \sqrt{2}\lambda_{d2})$  as shown by [5].

### C. Single-Mode Film Boiling

The interface is perturbed with  $y = y_c + A \cos(2\pi x / W)$ . The unperturbed height of the interface,  $y_c$ , is chosen to be  $0.125\lambda_{d2}$  and the amplitude of the cosine wave,  $A$ , is chosen to be  $-0.05\lambda_{d2}$ . Table I provides the thermo-physical properties for this test case.

TABLE I  
THERMO-PHYSICAL PROPERTIES OF FLUID USED IN SINGLE-MODE CASES

$T_{sat}$	$\rho_l / \rho_v$	$\mu_l / \mu_v$	$k_l / k_v$	$c_l / c_v$	$Pr_v$	$Gr$	$Ja$
625	4.78	2.59	3.56	0.66	4.39	17.93	0.071

The perturbed interface is contained in a domain of size  $(\lambda_{d2}, 3.6 \lambda_{d2})$ . Heavier fluid of density  $1.225 \text{ kg/m}^3$  is above

the interface, while the density of fluid below the interface is  $0.256 \text{ kg/m}^3$ . The domain width,  $W$ , and the number of modes of the perturbation ( $n_x$ ) are set such that their ratio is unity. The wall is fixed at a superheat of 15 K with the saturation temperature being 625 K. Fig. 2 shows the contours of vertical velocity at times 1 s, 7 s and 14 s. The interface location is shown by the black contour. At 7 and 14 s, acceleration of the liquid phase around the bubble results in increased necking of the bubble stem; the mushroom shaped cap breaks-off from the perturbed interface as the vapor film grows under the action of phase change.

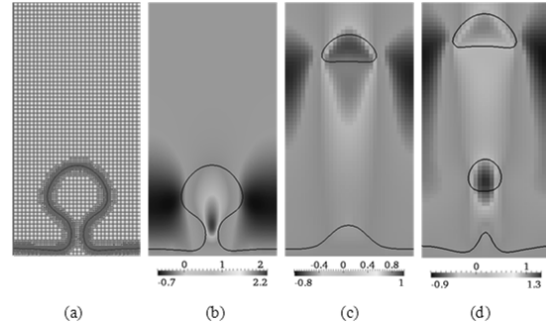


Fig. 2 2D single-mode film boiling: (a) Computational grid showing the refinement near the interface; Contours of vertical velocity at times (b) 1 s, (c) 7 s and (d) 14 s. The interface location has been superimposed as a black line. The fluid properties used correspond to the ones listed in TABLE I

### D. Bi-Modal Film Boiling

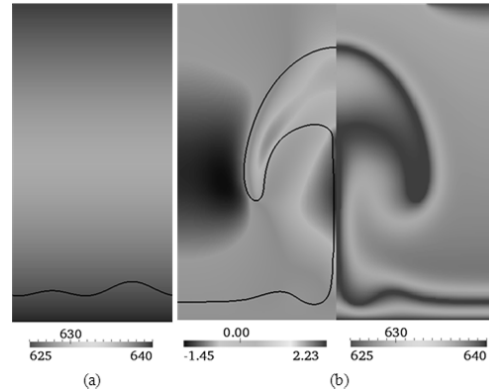


Fig. 3 Bi-modal film boiling: (a) Contours of mixture temperature at 0.0 s, (b) Contours of mixture velocity (m/s, left half) and mixture temperature (K, right half) at 2.0 s

A film boiling test case with a bi-modal initial perturbation is shown in Fig. 3 (a). The relevant properties/parameters are listed in Table I. Fig. 3 (b) shows the contours of mixture velocity (left half) and mixture temperature (right half) at 2.0 s. The interface location is shown by the solid black line. The superheated wall is specified at 640 K with a linear drop to the saturation temperature of 625 K at the top boundary. The prescribed perturbation generates a hydrostatic pressure difference between the crest and trough of the interface, which along with heat flux from the wall, leads to the formation of

mushroom shaped bubble.

#### E. Multi-Modal Film Boiling

In order to investigate the interaction of multiple modes in film boiling, a test case is studied with an initial perturbation of 30 random waves prescribed by:

$$y = y_c + (\varepsilon/N) \sum_{i=1}^N r(i) [\cos(2\pi i x/W) + \sin(2\pi i x/W)]. \quad (1)$$

Here,  $\varepsilon = -0.05\lambda_{d2}$ ,  $y_c = 0.125\lambda_{d2}$  and  $r(i)$  is a random number  $[0,1]$ . The initial interface shape is shown in Fig. 4 with a domain of size  $(10\lambda_{d2}, 2\lambda_{d2})$ . In addition to the perturbed interface, a second interface is specified at  $1.25\lambda_{d2}$ , which allows for the generated bubbles to "break through" and merge with a large body of vapor. The corresponding initial mixture temperature field is shown in Fig. 5.



Fig. 4 Initial interface shape for multi-mode film boiling (black – vapor; gray – liquid)

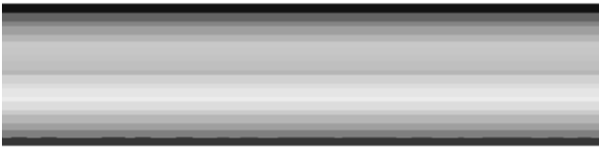


Fig. 5 Initial temperature field for multi-mode film boiling (black – 625 K; light gray – 640 K)



Fig. 6 Interface shape for multi-mode film boiling at 2 s (black – vapor; gray – liquid)

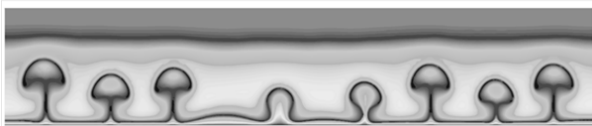


Fig. 7 Mixture temperature field for multi-mode film boiling at 2s (black – 625 K; light red – 640 K)

The interface shape and the corresponding mixture temperature field at 2s are shown in Fig. 6 and Fig. 7, respectively. The interface shape shows eight mushroom shaped bubbles that are growing/rising towards the flat second interface. Eventually, as the bubbles grow and interact with the interface they break-off as shown by the volume fraction

field and mixture temperature field at 4 s in Fig. 8 and Fig. 9, respectively.



Fig. 8 Interface shape for multi-mode film boiling at 4s (black – vapor; gray – liquid)

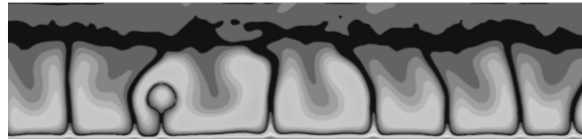


Fig. 9 Mixture temperature field for multi-mode film boiling at 4 s (black – 625 K; light gray – 640 K)

#### F. Three-Dimensional Film Boiling

A three-dimensional film boiling simulation is conducted in a domain of size  $(\lambda_{d3}, \lambda_{d3}, 1.3 \lambda_{d3})$ . The interface is perturbed with the following function:

$$z = z_c + A_x (\cos(2\pi m_x/W_x) + \sin(2\pi m_x/W_x)) + A_y (\cos(2\pi m_y/W_y) + \sin(2\pi m_y/W_y)). \quad (2)$$

In the above function,  $z_c = 0.125\lambda_{d3}$  is the unperturbed interface height, the maximum amplitudes in x and y directions are  $A_x = 0.018\lambda_{d3}$  and  $A_y = 0.036\lambda_{d3}$ , respectively. The perturbation modes in x and y directions ( $n_x$  and  $n_y$ ) are chosen to be 2.  $W_x$  and  $W_y$  denote the length and width of the domain, respectively.

Fig. 10 shows the (a) simulated vapor sheet and vertical velocity vectors and (b) the corresponding octree grid at 1.15 s. A mushroom shaped vapor bubble is seen to evolve at the center of the domain. This test case clearly demonstrates the robustness of the adaptive calculations to simulate full three-dimensional film boiling and provides an efficient and feasible tool to study multi-modal film boiling.

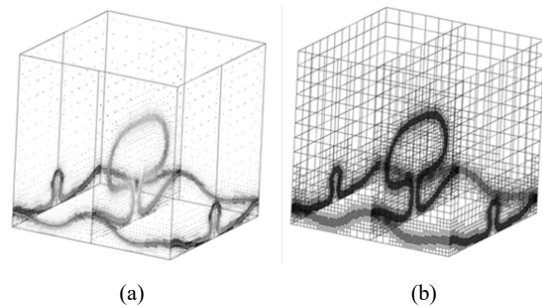


Fig. 10 Three-dimensional film boiling: (a) contours of volume fraction and vertical velocity vectors and (b) corresponding octree grid at 1.15 s for bimodal initial perturbations

## VI. CONCLUSION

A robust phase change model developed on octree grids is used to conduct single and multi-modal film boiling simulations. The phase change model is developed using the VOF framework accounting for mass, momentum and energy exchange between the phases. Different aspects of the model are validated including simulation of instability growth under normal gravity conditions, time reversed advection, and ability to simulate bubble growth rates on adaptive octree grids. Finally, instability growth with phase change (film boiling) on adaptive grids is simulated to demonstrate the ability of the method to simulate complex problems in an efficient and accurate manner.

Single and multi-mode film boiling simulations on flat horizontal surfaces are conducted on two and three-dimensional adaptive grids. The use of octree grids allows conducting such simulations with high fidelity near the interface while maintaining a much coarser grid away from the interface (typically 3 to 4 levels of refinement coarser) and the wall allowing for more reasonable simulation times. This work provides an efficient and accurate platform to conduct multi-modal film boiling simulations, which has the ability to show the complex interaction of multi-modes leading to more realistic boiling flow simulations.

## ACKNOWLEDGMENT

The author acknowledges the administrative support from the staff of the Center for Advanced Computing and Data System (CACDS).

## REFERENCES

- [1] M. W. Akhtar and S. J. Kleis, "A volume of fluid phase change model on adaptive octree grids," *Journal of ASTM International*, vol. 8 no. 3, pp. 1–21, 2011.
- [2] J. U. Brackbill, D. B. Kothe, and C. Zemach, "A continuum method for modeling surface-tension," *J. Comput. Phys.*, vol. 100, no. 2, pp. 335–354, 1992.
- [3] M. W. Akhtar. and S. J. Kleis, "Boiling flow simulations on adaptive octree grids," *Int. J. of Multiphase Flow*, vol. 53, pp. 88–99, 2013.
- [4] B. A. Nichita, *An Improved CFD Tool to Simulate Adiabatic and Diabtic Two-Phase Flows* PhD. Dissertation. École Polytechnique Federale De Lausanne, 2010.
- [5] Y. J. Lao, R. E. Barry, R. E. Balzhiser, "A study of film boiling on a horizontal plate," Paper B3.10, *Fourth International Heat Transfer Conference*, Paris, Versailles ("Heat Transfer 1970" vol. V, Elsevier, Amsterdam).